



Numerical Study of Panel Zone in a Moment Connection without Continuity Plates

Alireza Rezaeian, Ebrahim Jahanbakhti & Nader Fanaie

To cite this article: Alireza Rezaeian, Ebrahim Jahanbakhti & Nader Fanaie (2020): Numerical Study of Panel Zone in a Moment Connection without Continuity Plates, Journal of Earthquake Engineering, DOI: [10.1080/13632469.2019.1695021](https://doi.org/10.1080/13632469.2019.1695021)

To link to this article: <https://doi.org/10.1080/13632469.2019.1695021>



Published online: 17 Feb 2020.



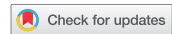
Submit your article to this journal [↗](#)



View related articles [↗](#)



View Crossmark data [↗](#)



Numerical Study of Panel Zone in a Moment Connection without Continuity Plates

Alireza Rezaeian^a, Ebrahim Jahanbakhti^b, and Nader Fanaie^b

^aDepartment of Civil Engineering, Karaj Branch Islamic Azad University, Karaj, Iran; ^bDepartment of Civil Engineering, K. N. Toosi University of Technology, Tehran, Iran

ABSTRACT

Built-up box columns are more frequently used in earthquake-prone regions such as Japan and Iran. As the installation process of continuity plates and welding inspection are difficult, expensive, and time-consuming, this study was aimed at experimentally and numerically investigating continuity plate elimination from built-up box columns with regard to the seismic design specifications of special and intermediate moment resisting frames. Results of an experimental study of three full-scale rigid connections between I-beam and box-column subjected to cyclic loading were used for comparison and verification of numerical results. Experimental study showed that samples reached story drift angle of 0.06 radians before experiencing the permissible strength degradation. Therefore, the tested connections satisfied the criterion for special moment resisting frame (SMRF) in AISC. Based on observations of crack initiation and propagation in the experimental study, a rupture index (RI) was employed to investigate the effects of different complete joint penetration (CJP) groove welding methods used in the experimental study on connection ductility as well as to identify the regions prone to crack initiation and propagation. Both the numerical and experimental results showed the superiority of using back plate in CJP welding.

ARTICLE HISTORY

Received 22 October 2018
Accepted 15 November 2019

KEYWORDS

Numerical study; moment connection; continuity plate; built-up box column; seismic design

1. Introduction

Built-up box columns have acceptable seismic behavior owing to noticeable moment capacity about each axis, high torsional stiffness, and low sensitivity to local buckling. Providing a proper connection between box column and beam is indispensable for achieving the merits of box column in a moment frame. Considering the strong column-weak beam criterion, different beam to box-column connections have been investigated. Continuity plates have a considerable influence on the seismic behavior of box columns from the perspective of ductility and stable hysteretic properties (Castro, Dávila-Arbona, and Elghazouli 2008). In what follows, some research studies on this subject are presented.

Local buckling phenomenon usually impedes the development of highly dissipative mechanisms in both column web and plates in compression. Accordingly, the use of stiffeners, such as continuity plates, is commonly suggested (Latour, Piluso, and Rizzano 2011). Applying a couple of continuity plates with a thickness equal to the beam flange thickness assures maintaining the column web in the elastic range (Iannone et al. 2011) and leads to transferring the beam load to

the column through the panel zone as well as utilizing the whole capacity of the panel zone. Several experimental and numerical studies have been conducted to identify the requirement of continuity plates and the possibility of their substitution by external stiffeners. Due to difficulties of fabrication as well as the costly procedure of installing the internal continuity plates, researchers have tried to improve this type of connection in the presence and absence of internal continuity plates. In the presence of internal continuity plates, improving the connection details has been recently addressed by horizontal hunch connection (Tanaka 2003), column-tree connection with improved details including widened flange of the stub beam detail (Chen, Lin, and Lin 2006), and rib-reinforced welded connections (Chen, Lin, and Tsai 2004). However, in the absence of internal continuity plates, this type of connection can be improved by providing new load paths via external features using external T-angle or triangular plate stiffeners for box-columns (Shanmugam and Ting 1991, 1995) and concrete-filled tubular (CFT) columns (Kang et al. 2001; Shin, Kim, and Oh 2008), collar stiffening plates around the box-column (Kurobane 2002; Park, Kang, and Yang 2005), connection with high-strength blind bolts (Korol, Ghobarah, and Mourad 1993), and moment end-plate connections (Wheeler, Clarke, and Hancock 2001; Wheeler et al. 1998). Ricles et al. (2002) used non-linear finite element models for full-scale I-beam to H-shape column connections so as to investigate the effects of weld metal, continuity plates, beam web attachment, weld access hole geometry, and panel zone strength on cyclic ductility. They developed improved details for welded unreinforced connections as well. Based on their results, continuity plates are not necessarily required when plastic story drift angles are greater than 0.041 radians for the specimens without continuity plates. Chen, Lin, and Tsai (2004) experimentally and analytically investigated the cyclic behavior of connection between steel beam and welded box column reinforced by vertical rib plates located on the beam flanges. The specimens experienced inelastic rotations more than 0.03 radians, and a plastic hinge was formed in the beam far from the column interface. They concluded that utilizing the welding diaphragm inside the box column was crucial in transferring the forces from beam to the connection. Kim et al. investigated moment transfer efficiency of connections through non-linear finite element analysis (FEA) of five connection models. According to their results, moment transfer efficiency of the connections with box columns was not comparable with that of H-columns (Kim and Oh 2007). Goswami and Murty (2010) analytically investigated a proposed connection using external reinforcement rather than continuity plates in the I-beam to box-column seismic connection. The obtained results showed that the plastic hinge was pushed away from the column face. Moreover, it was not necessary to connect beam web to column flange since the entire shear was directly transferred toward column webs through beam flange using stiffeners. Ghobadi et al. (2009) investigated experimentally and analytically a developed connection between I-beam and box column using horizontal T-stiffeners. According to their experimental tests, story drift angle could reach 0.06 radians prior to experiencing 20% strength degradation and crack propagation. On the other hand, based on their analytical study, the potential of crack initiation was reduced using fillet weld instead of complete joint penetration (CJP) groove weld for connecting T-stiffener to beam flange. Chou and Jao (2010) conducted experimental and analytical investigations into five steel I-beam to box-column connections rehabilitated by internal beam flange stiffeners. According to the obtained results, the capacity-demand ratios between 1.0 and 1.1 could be considered as the minimum requirement for seismic design of such connections. Moreover, rupture index (RI) was significantly reduced by increasing the thickness or depth of internal beam flange stiffeners. Kiamanesh, Abolmaali, and Ghassemieh (2010) investigated the effects of stiffeners and column

flange thickness on the performance and energy dissipation of the connection, experimentally and analytically. They assessed the effects of stiffeners on hysteresis curve, load transfer mechanism, and stress and strain patterns of the connections using 20 finite element models. Mirghaderi, Torabian, and Keshavarzi (2010) and Torabian, Mirghaderi, and Keshavarzi (2012) proposed a new moment connection for connecting I-beam to box-column applying for vertical plates instead of continuity plates. The connection was investigated passing a vertical plate through: (a) symmetry axis and (b) diagonal axes of a square box-column. They subjected two specimens under cyclic loading and suggested a design method for calculating plate dimensions as well as evaluating the seismic performance of their proposed connection. The specimens reached at least a total story drift angle of 0.06 radians before experiencing strength degradation. Therefore, the proposed connection was prequalified for special moment-resisting frames (SMRFs). Saneei Nia, Ghassemieh, and Mazroi (2013) experimentally and analytically studied the seismic performance of three full-scale I-beam to box-column welded unreinforced flange-welded web (WUF-W) connections. The results displayed that this type of connection to the box column could satisfy the SMRFs criterion. The box columns were also investigated analytically under biaxial bending.

Up to now, limited studies have been carried out on box columns. Regarding the wide use of these columns in some countries as well as the difficulties of continuity plate installation¹ and welding inspections, the possibility of eliminating continuity plates is investigated in this study by increasing the column flange thickness. An equation to specify the need for continuity plates in box columns has previously been evaluated by an experimental study (Jahanbakhti, Fanaie, and Rezaeian 2017). A verified numerical model based on the experimental results is presented in this study which is employed to investigate the I-beam to Box-column moment connection without continuity plates. In a rigid connection, panel zone plays an important role in transferring the compression and tension loads from beam flanges to column flanges. In this regard, numerical results are investigated to realize the load transfer mechanism from beam to column and the behavior of the panel zone in the absence of continuity plates. According to the experimental observation of crack initiation and propagation during the cyclic loading test, local behavior and ductility in the connection region of beam flange to column flange are investigated. Moreover, crack propagation is numerically estimated by extracting local stress and strain from the results and using an RI which is introduced below.

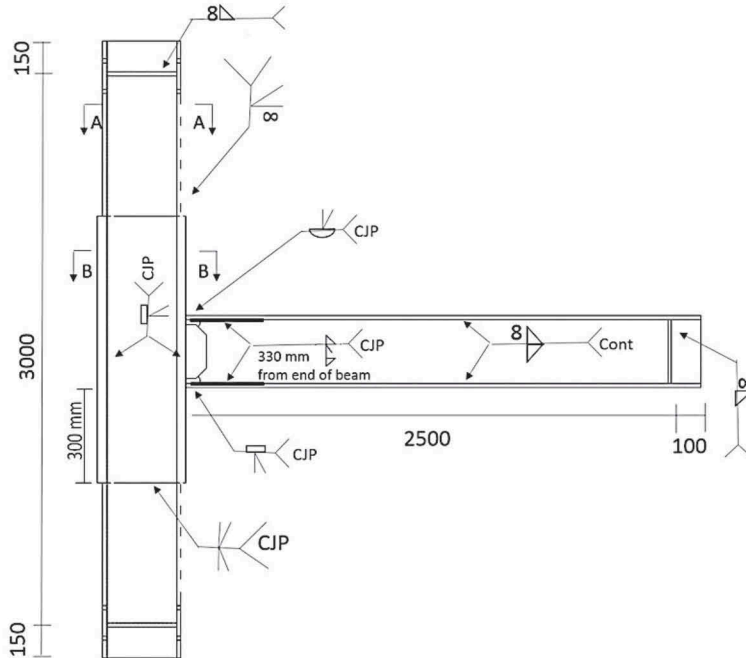
2. Purpose and Methodology of the Study

Based on analytical and experimental study of the possibility of continuity plate elimination from moment connection of I-beam to built-up box column, Eq. (1) is proposed (Jahanbakhti, Fanaie, and Rezaeian 2017). Three full-scale connections with details presented in Table 1 and Fig. 1 are used in the experimental study. A prequalified WUF-W

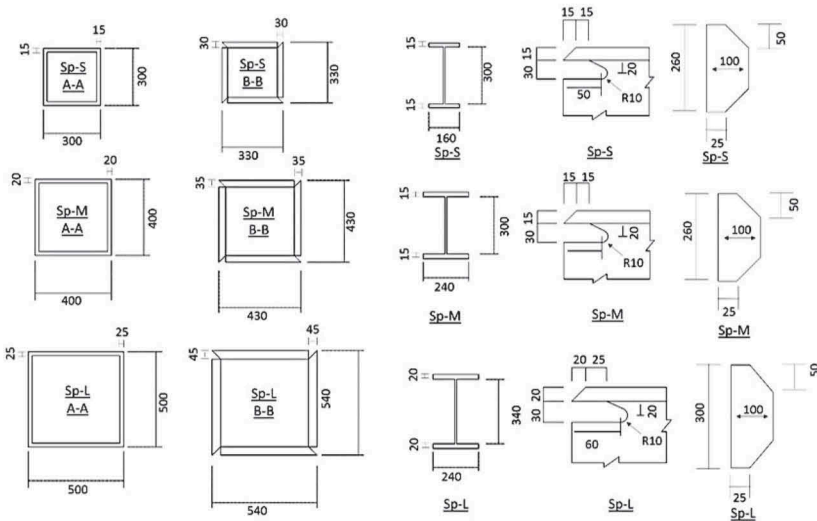
¹For building-up a box column reinforced with continuity plates, a U-shaped section is built first. Then, a continuity plate is welded to three plates using full penetration groove weld. The prepared U-shaped section is covered and welded by a plate with limit length as the fourth side of the box column. The continuity plate is welded to the fourth side of box column by welder, manually. These fourth sides of box column are welded to the U-shaped section at the level of each story, and finally, the parts not covered are completed and welded. Another approach to welding continuity plates inside a tubular column is electro-slag welding, which welds the continuity plates to the fourth side automatically. A laser technology for innovative connections in steel constructions is RFCS LASTEICON, which is a new method. Due to sanctions, this technology is not available in Iran.

Table 1. List of analytical investigations (unit: mm) (Jahanbakhti, Fanaie, and Rezaeian 2017).

Specimen	Box-column (mid-part)	Box-column (side-part)	I-beam
Sp-S	330 × 330 × 30	300 × 300 × 15	160 × 330 × 8 × 15
Sp-M	430 × 430 × 35	400 × 400 × 20	240 × 330 × 8 × 15
Sp-L	540 × 540 × 45	500 × 500 × 25	240 × 380 × 8 × 20



(a)



(b)

Figure 1. Experimentally tested specimens: (a) connection details and (b) section details (Jahanbakhti, Fanaie, and Rezaeian 2017).

connection without continuity plates and increased column flange thickness satisfying Eq. (1) (Jahanbakhti, Fanaie, and Rezaeian 2017) was employed for the specimens. Complete joint I penetration groove welding and partial penetration groove welding were used for the panel zone and both sides of the column, respectively. Full CJP groove welding was employed to connect I-beam to built-up box-column flange. Beam web was connected to beam flanges with CJP groove welding at a distance of 400 mm from column face, and then, fillet welding was used at the end of the beam. Test setup included simple support of both sides of the column and lateral bracing in the middle and at the free end of the beam (Fig. 2). Displacement-controlled cyclic loading (Fig. 3) was applied to the free end of the beam according to AISC-341-10 (2010) loading protocol.

$$t_{cf} \cong 0.4 \sqrt{1.3 \left(1.8 t_{bf} b_{bf} \frac{F_{yb}}{F_{yc}} \right)} = 0.46 \sqrt{1.8 t_{bf} b_{bf} \frac{F_{yb}}{F_{yc}}}, \quad (1)$$

where t_{cf} , t_{bf} , b_{bf} , F_{yb} and F_{yc} are column flange thickness, beam flange thickness, beam flange width, beam flange yield strength, and column flange yield strength, respectively.

Moment-drift angle hysteresis diagrams of three tested specimens are depicted in Fig. 4. In all specimens, flexural strength in drift angle of 0.04 radians is higher than the nominal

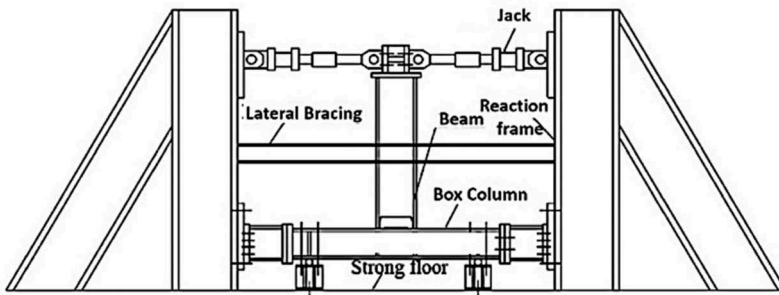


Figure 2. Laboratory test set-up (Jahanbakhti, Fanaie, and Rezaeian 2017).

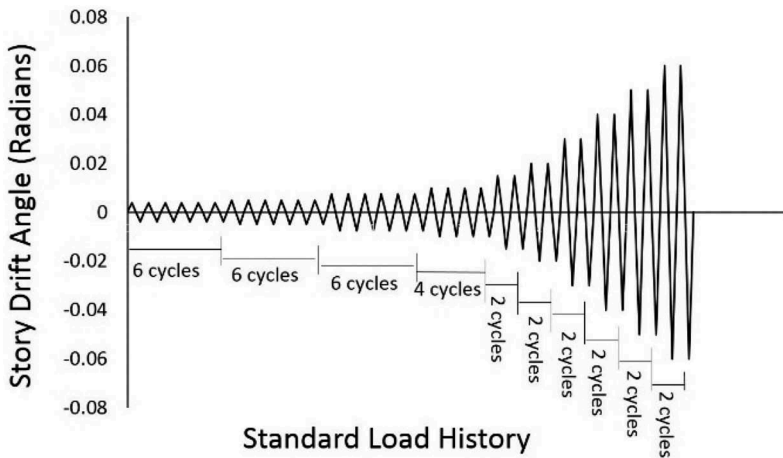


Figure 3. Cyclic loading protocol of AISC-341-10.

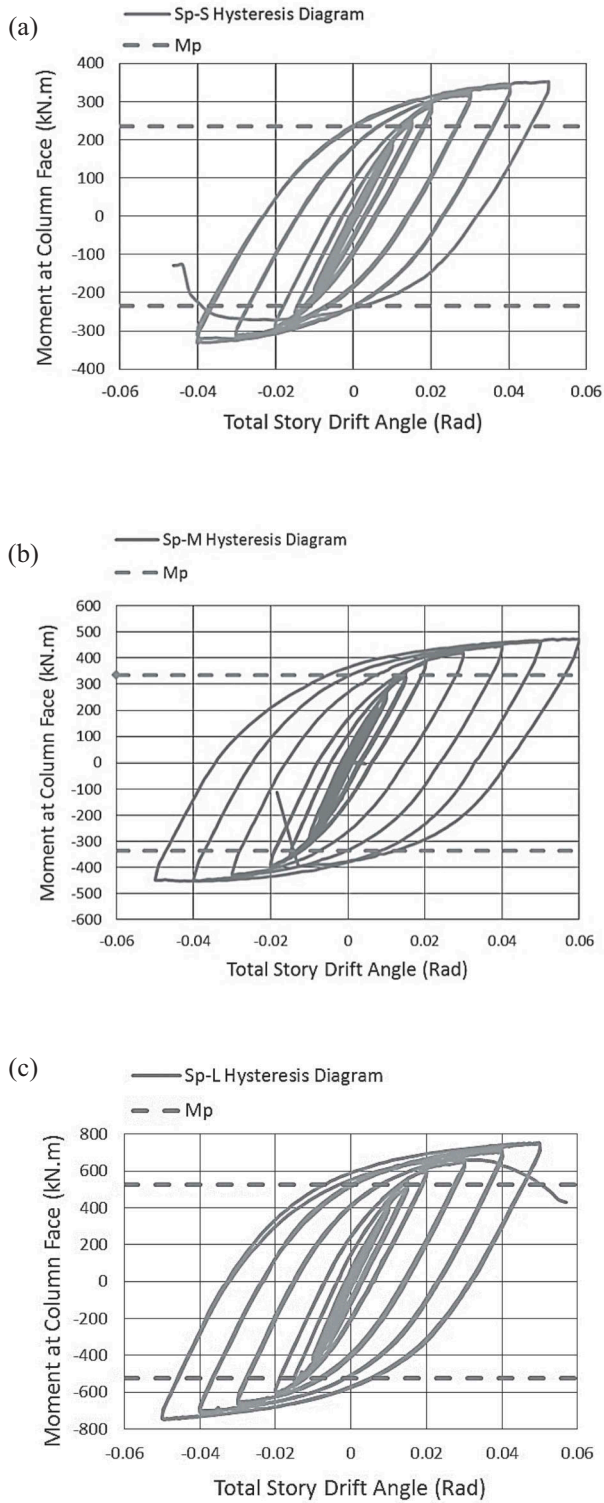


Figure 4. Hysteresis curves for experimentally tested samples: (a) specimen Sp-S, (b) specimen Sp-M, and (c) specimen Sp-L (Mp: nominal flexural strength) (Jahanbakhti, Fanaie, and Rezaeian 2017).

flexural strength (M_p) shown by horizontal dashed line. According to the acceptance criterion of strength degradation in AISC-341-10 seismic provision (flexural strength at drift angle of 0.04 radians should not be less than 80% nominal flexural strength), all the specimens satisfy the acceptance criterion of SMRF.

According to the test results, nonlinear behavior begins at the story drift angle of 0.0075 radians, and crack initiation is observed at the story drift angle of 0.04 radians. Crack initiation and propagation is observed in both types of CJP groove welding between the beam flanges and column flange as shown in Fig. 1a. The connection finally fails and separates from the CJP groove weld with 8 mm fillet back weld. Using a back plate in CJP groove welding results in better ductility for the connection.

3. Numerical Studies

3.1. Finite Element Model

3D finite element analyses were employed to verify numerical models by experimental results and numerical studies. ABAQUS software was utilized to conduct nonlinear analyses in terms of material and geometry. According to experimental studies of laboratory tested I-beam to box-column connections without continuity plates under cyclic loading, the list and geometry of numerical models are presented in Table 1. The connections are of prequalified WUF-W type, as shown in Fig. 1. The geometries of numerical models are based on the dimensions in the experimental studies. Weld elements are modeled with approximate dimensions and a tie constraint between connected surfaces is employed to provide a welded connection (tie constraint is used to tie up all of the nodes in fixed connection with each other).

In each laboratory tested specimen, the column is connected to strong floor with simply supported bearings, as presented in Fig. 2. The beam is laterally braced at the distances of 1200 and 2500 mm from the column face. The actuator is set up at the distance of 2500 mm from the column face at the end of the beam to apply AISC-341-10 cyclic loading protocol (Fig. 3). Then, as shown in Fig. 6, in each numerical model, the column is restrained by simple support at both sides. Also, the beam is braced laterally at the distance of 1200 mm from column face at the end of the beam, where cyclic loading is applied based on AISC-341-10 loading protocol. A three-dimensional numerical model is generated using the 20-node quadratic/cubic brick elements (C3D20R), which are proper for plasticity and large deformation (with three translational and rotational degrees of freedom for each node). Also, mesh sizes of 40 mm for beam elements and 50 mm for column elements (considering mesh convergence study) are considered to investigate the cyclic behavior of connection, plastic hinge, and panel zone. A tie constraint is used to connect the beam to column flange. Bilinear stress–strain relationship, as shown in Fig. 5, is considered to define the nonlinear behavior of materials (bilinear model is employed to capture strain hardening of steel). In this regard, Young's modulus of $E = 210$ GPa and Poisson's ratio of $\nu = 0.3$ are considered for all connection components in the elastic region. Stress–strain variation between yield strength (F_y) and ultimate strength (F_u) is assumed linear with the slope of $0.06 E$ (slope of stress–strain diagram in the plastic region is generally considered between 1% and 10% of elasticity modulus). Kinematic hardening is assumed as well. No material fracture has been reported in the experimental study; accordingly, no fracture property is considered for materials. Yield and ultimate stresses of each plate used in the experimental test have been

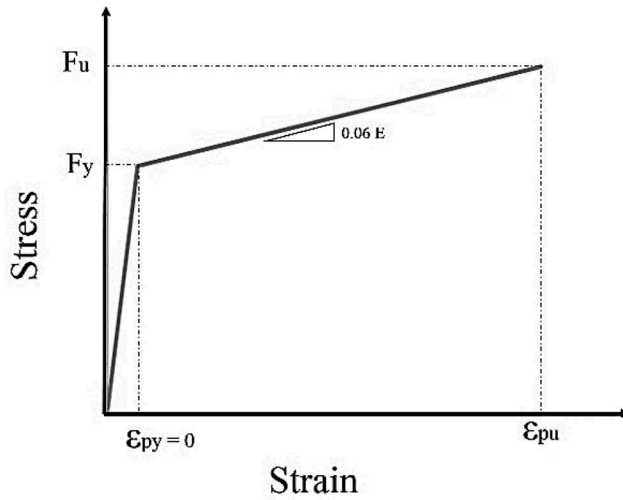


Figure 5. Stress–strain diagram of modeled steel.

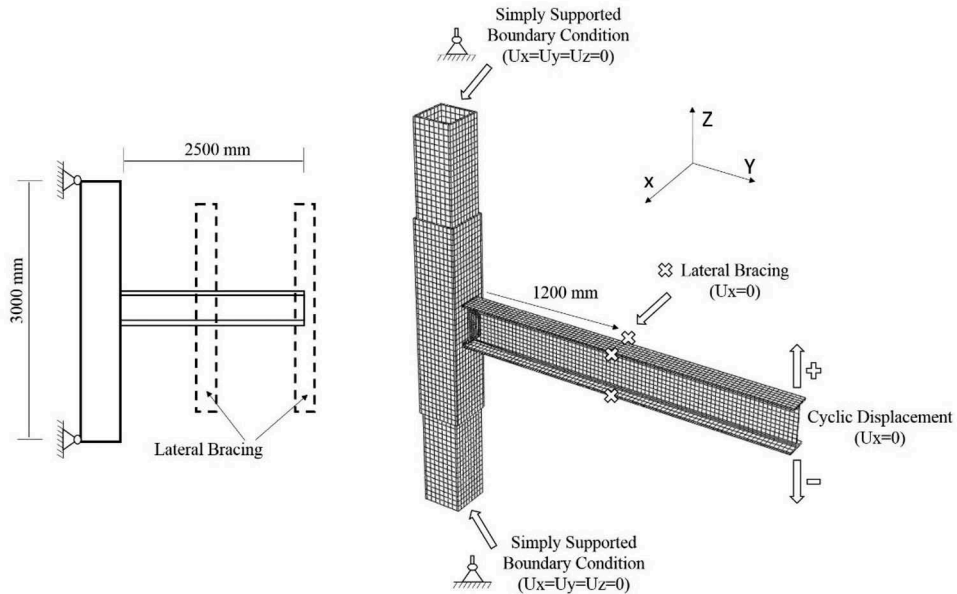


Figure 6. Finite element model and boundary conditions.

obtained by coupon test, and the results are presented in [Table 2](#) (Jahanbakhti, Fanaie, and Rezaeian 2017). Fracture strain is considered from 0.260 to 0.282 based on coupon tests for different thicknesses. Weld material is modeled according to the mechanical specifications presented by the manufacturer ([Table 3](#)). [Fig. 6](#) illustrates the numerical model and boundary conditions for specimen Sp-S. Based on the test loading and contact elements, static general analysis method has been employed. The presented numerical model in this paper is constituted after several tries and considering different methods of modeling to find the best reliable model.

Table 2. Mechanical specifications of the plates used in construction (Jahanbakhti, Fanaie, and Rezaeian 2017).

Specimen	Part	F_y (MPa)	F_u (MPa)	Elongation (%)
Sp-S	Beam web	289.5	382.3	27.7
	Beam flange	250.0	379.1	28.2
	Column web and flange (mid part)	259.0	412.4	27.2
	Column web and flange (side part)	250.0	379.1	28.2
Sp-M	Beam web	289.5	382.3	27.7
	Beam flange	250.0	379.1	28.2
	Column web and flange (mid part)	282.0	461.3	26.4
	Column web and flange (side part)	268.0	381.9	26.5
Sp-L	Beam web	289.5	382.3	27.7
	Beam flange	268.0	381.9	26.5
	Column web and flange (mid part)	280.0	390.4	26.0
	Column web and flange (side part)	272.5	442.1	25.8

Table 3. Mechanical specifications of beam to column connecting welds (ER70S-6 Electrode (www.weldwire.net, 2016)).

Material	F_y (MPa)	F_u (MPa)
Weld	430	540

3.2. Verification of Finite Element Model

Fig. 7 illustrates the hysteresis curves plotted for the modeled specimens obtained by FEA and those obtained from experimental tests up to failure point. Based on this figure, ultimate load and stiffness are well predicted, and suitable agreement is evident between the analytical and experimental results in the hysteresis loops. According to Fig. 8, deformation of the tested specimens and the results of numerical analysis show good agreement in similar drifts. Employing a quadratic mesh type for beam flange (proper to capture plastic strain and large deformation as well as stress concentration) by considering residual plastic deformation in presence of compression load on beam flange leads to an out-of-plane deformation at plastic hinge, which is different from local buckling. This out-of-plane deformation is shown in the results of the numerical analysis (Fig. 8). Thus, finite element model is verified by using experimental results. The provided finite element model is capable of analyzing and predicting the seismic performance of rigid connection of I-beam to box-column without continuity plates.

The discrepancies between the results of FEA and those of experimental tests are due to the geometric difference, the exact boundary condition properties, uncertainties in the model of mechanical behavior of the materials, residual stresses, etc.

4. Response Index

To investigate and compare the ductile failure potential of different analyzed connections, an RI is computed for each node of the connections using Eq. (2) (Ricles et al. 2002) considering the availability of verified finite element models of rigid connections between I-beam and box-column with and without continuity plates. Accordingly, the described RI is also used to investigate crack propagation in two types of CJP grooves used in the experimental tests, which have relatively different reported behaviors.

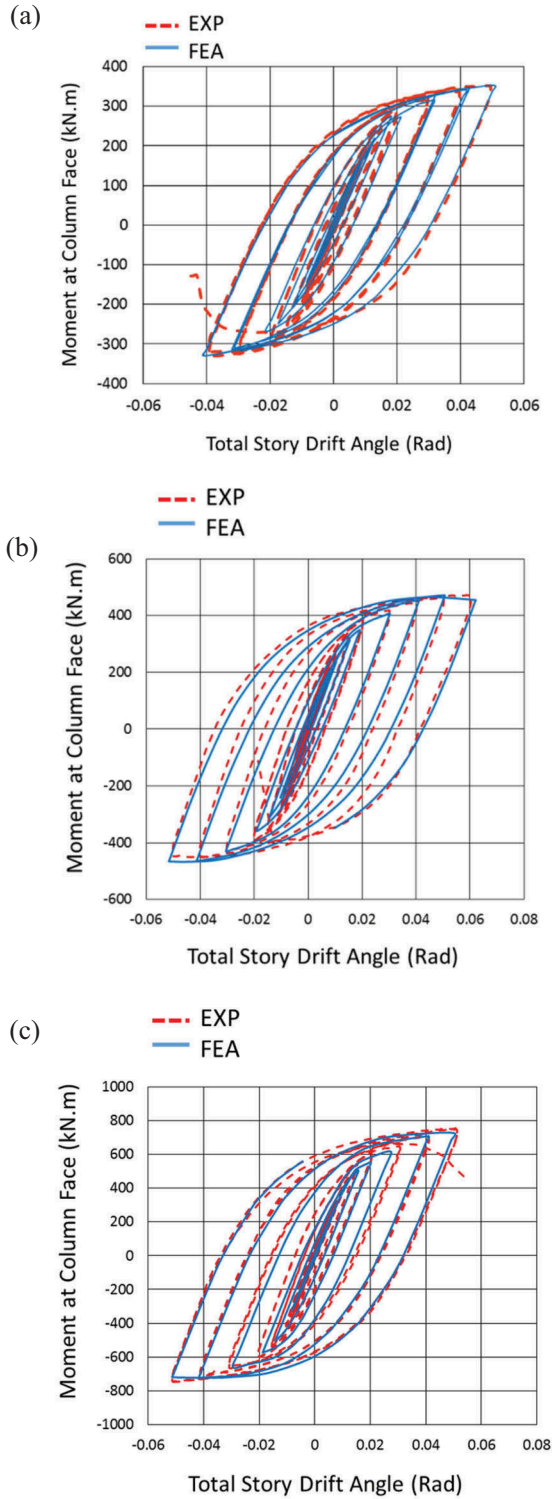


Figure 7. FEA and experimental hysteresis diagrams: (a) specimen Sp-S, (b) specimen Sp-M, and (c) specimen Sp-L.

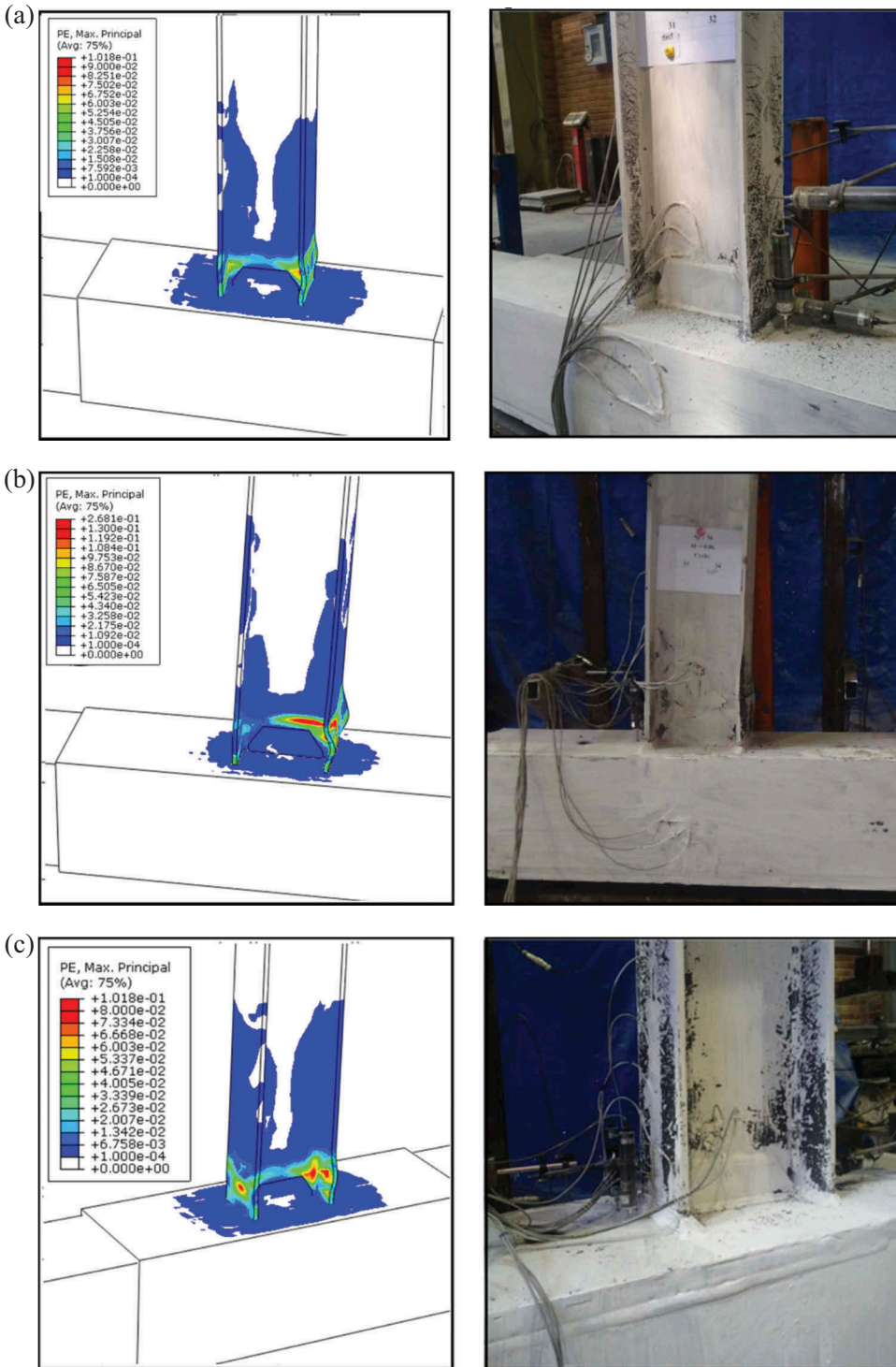


Figure 8. Numerical analysis and experimental test of plastic strain and deformation: (a) specimen Sp-S at 5% radian, (b) specimen Sp-M at 6% radian, and (c) specimen Sp-L at 5% radian.

$$RI = \frac{PEEQ}{\exp\left(-1.5 \frac{\sigma_m}{\sigma_{eff}}\right)}, \quad (2)$$

where PEEQ is equivalent plastic strain, σ_m is hydrostatic stress, and σ_{eff} is von Mises stress (Ricles et al. 2002).

4.1. Ductility Failure Potential in Absence of Continuity Plates

Concerning the similarity of experimentally tested specimens with continuity plates by Saneei Nia et al. and experimentally tested specimens without continuity plates (Jahanbakhti, Fanaie, and Rezaeian 2017), the ductility potential of moment-resisting connection is investigated in the absence of continuity plates. The comparison is carried out with the same dimension, beam to column connection, and boundary condition for both specimens of Saneei Nia et al. tests and Jahanbakhti et al. tests. Table 4 presents the values of RI reported by Saneei Nia et al. as well as those obtained in this research. Weld metal was not modeled in Saneei Nia et al.'s finite element model of connection, and values of von Mises stress, hydrostatic pressures, and equivalent plastic strain for points A and B in Fig. 9a were used to compute the values of RI. Here, the finite

Table 4. PEEQ, von Mises stress, and hydrostatic pressure at total story drift angle of 0.06 radians for different specimens.

Specimen	Point	PEEQ	With continuity plates [10]			Without continuity plates			
			von Mises stress (MPa)	Hydrostatic stress (MPa)	RI	PEEQ	von Mises stress (MPa)	Hydrostatic stress (MPa)	RI
Sp-S (DC-S) ^a	A	1.18	326.5	267.7	4.0	3.5	339.2	315.5	14.1
	B	0.96	374.7	305.1	3.2	4	354.3	327.1	15.9
Sp-M (DC-M) ^a	A	0.91	392.7	150.6	1.6	3.5	329.1	252.6	11.0
	B	1.10	391.4	177.3	2.2	2.8	328.8	296.2	10.8
Sp-L (DC-L) ^a	A	1.75	349.4	310.4	6.3	2.7	318.2	307.2	11.5
	B	1.53	363.1	327.1	5.9	2.5	350.3	269.3	7.9

^aDC-S, DC-M, and DC-L represent the names of specimens in the study done by Saneei Nia et al.

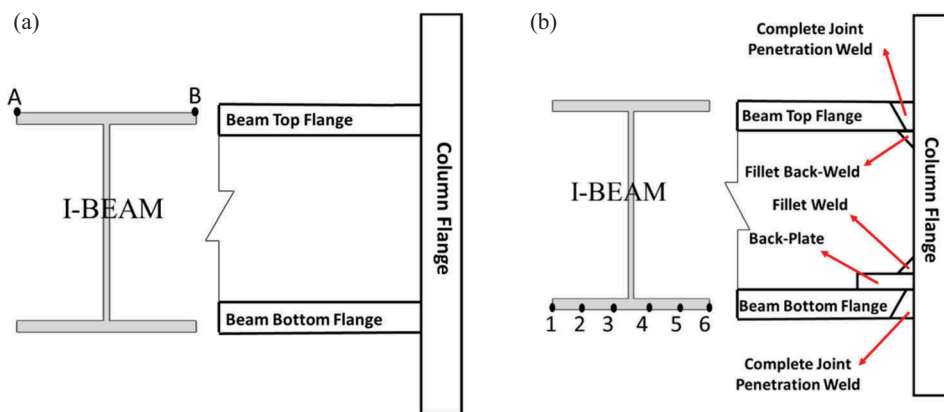


Figure 9. Selected nodes from numerical results to get the PEEQ, von Mises stress, and hydrostatic pressure: (a) direct connection between beam and column, and (b) indirect connection between beam and column (modeling weld material).

element models verified in Sec. 3.2 are applied without modeling the weld metal. Beam section, including flanges and web, is directly tied to column flange, and the values required for calculating RI are taken from similar points (A and B). Comparing the values of RI obtained for rigid connections of I-beam to built-up box column without and with continuity plates shows the increases of 290%, 410%, and 170% for the connections Sp-S, Sp-M, and Sp-L, respectively. These increases in RI for the connections without continuity plates prove that there is a lower ductility capacity in the absence of continuity plate than in its presence.

4.2. Ductility Failure Potential in Different Types of Welding Processes

Fig. 1 presents two types of CJP groove welds in the connection regions of beam flanges to column flanges. The finite element models presented in Sec. 2 are used for the new numerical modeling by considering the aforementioned welds and verified by the experimental results similar to the previous model. Damage of welds is not considered in the finite element modeling in this research. Weld elements are modeled as separate parts, and connecting surfaces between weld elements and other frame elements are constrained using tie constraint. ABAQUS provides a tie constraint on all constrained degrees of freedom from each node to the other node, which are tied together. Based on the experimental reports, the connections are finally fractured from the region of beam flange to column flange connection (in groove weld of upper beam flange to the column flange) created by the back weld method. The values of von Mises stress, hydrostatic pressure, and equivalent plastic strain are presented in Fig. 9b for the nodes with the numbers 1–6. These values correspond to the connection region of beam flange at a drift angle of 0.06 radians. Table 5 presents two types of CJP groove welds with back plates (the plates with 8 mm thickness) and with backing fillet weld for Sp-S finite element specimen. According to Fig. 10, the values of RI are about 5–10% higher on the edges for the fillet weld as backing than for the back plate.

4.3. Panel Zone Behavior

In the moment-resisting frame, as expected, plastic hinge is formed near the column face at the beam. Plastic moment and plastic shear force are transferred to the column by means of beam flanges and web. Beam flanges and beam web transfer the tensile and compressive forces resulting from the moment and beam shear force to the column flange, respectively. As shown in Fig. 11, the force transferred from beam flange goes to the continuity plates. This normally transferred force goes to the box-column webs in the form of shear force. By restraining the

Table 5. PEEQ, von Mises stress, and hydrostatic pressure at total story drift angle of 0.06 radians for different welding processes.

Specimen	Point	PEEQ	Back weld		Back plates		
			von Mises stress (MPa)	Hydrostatic stress (MPa)	PEEQ	von Mises stress (MPa)	Hydrostatic stress (MPa)
Sp-S	1	3.4	343.6	-287.7	3.7	346.4	-311.3
	2	2.9	349.8	-382.9	2.8	349.9	-425
	3	1.6	349.7	-263.3	1.5	350.6	-278.3
	4	1.2	350.2	-307.5	1.3	350.9	-296.7
	5	1.6	348.1	-286.5	1.9	349.6	-419.5
	6	2.3	350.9	-290.4	2.7	347.6	-339.9

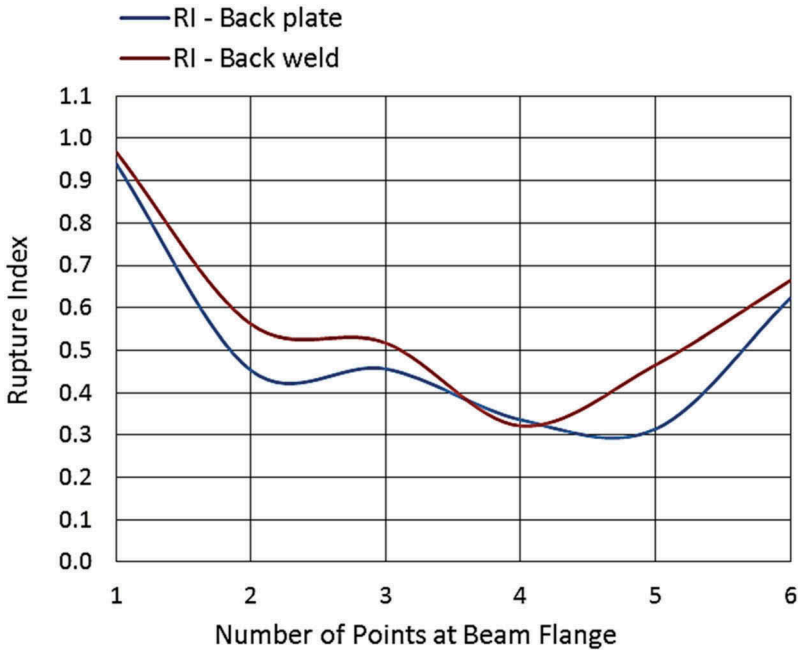


Figure 10. RI through beam flange width in Sp-S specimen.

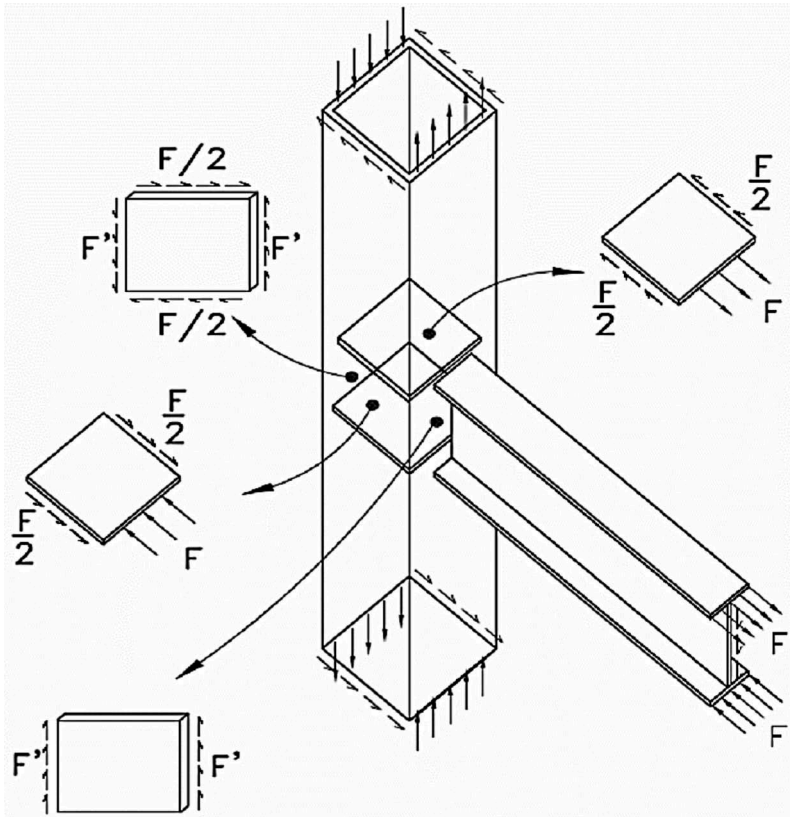


Figure 11. Force transferring path.

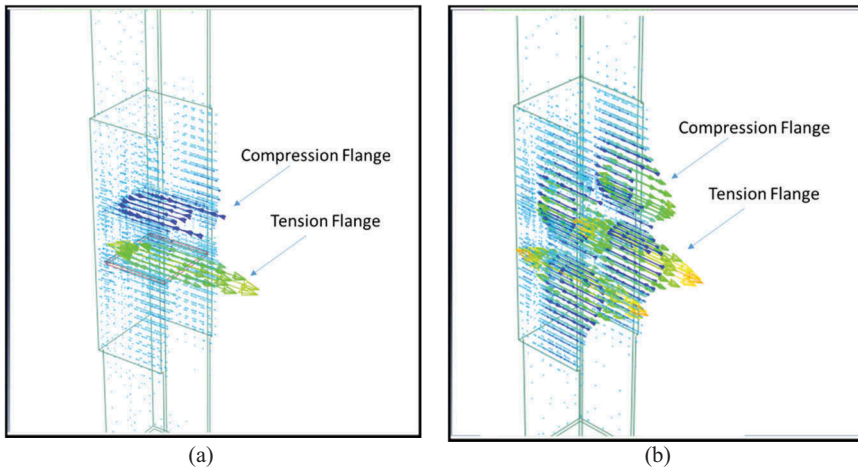


Figure 12. Stresses distribution (Pa) through beam flanges in a box-column: (a) with continuity plates and (b) without continuity plates.

vertical sides of the web by column flange, direction of shear force in the panel zone changes. Finally, it results in the axial forces in the column flanges and produces a bending moment in the column section (Mirghaderi and Moradi 2006). Fig. 12 shows the transfer path of force from beam to panel zone for both types of connections, with and without continuity plates, through plotting stress vectors in the panel zone in the direction of beam axis. Beam and column flange are omitted in Fig. 12 for more clarity of stress vectors.

Vectors of existing stresses in three regions of the column, namely (a) in the middle of panel zone, (b) exactly above the connection of beam flange to column flange (above the continuity plate) for both connections (with and without continuity plates), and (c) slightly above the panel zone, are used to investigate the load transfer mechanism. Vectors of existing stresses in the cross-section of the column, in the direction of the column axis, for the mentioned three regions are shown in Figs. 13–15. Fig. 13a shows a concentrated moment on the column flange

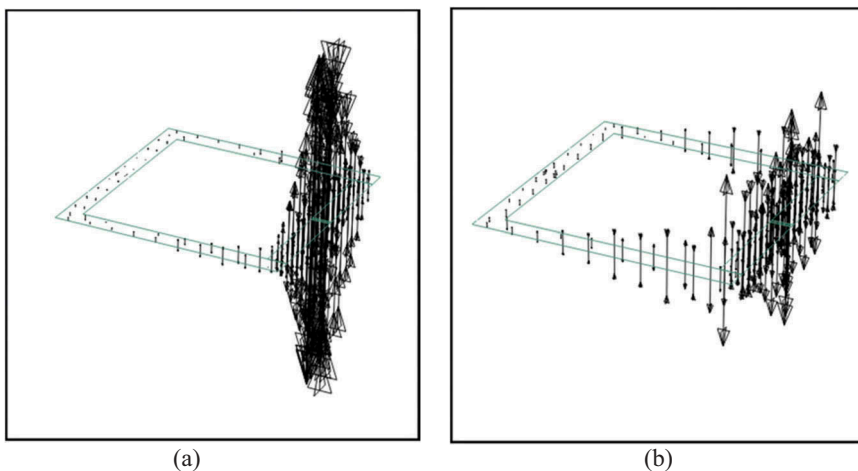


Figure 13. Stress (Pa) through column flanges for specimen Sp-L in the middle of the panel zone of one-way I-beam to box-column connection: (a) with continuity plates and (b) without continuity plates.

in the middle of the panel zone with continuity plates. According to Fig. 14b, in the connections without continuity plates, concentrated and relatively high moment is applied to the column flange in its connection to the beam flange. Fig. 15 shows the tensile and compressive behaviors of column flange in both connections after transferring moment from beam to column by panel zone. Based on the figures, the stress is more uniformly distributed on the cross-section of the column in connection with continuity plates. Figs. 12–15 depict the force transmission path in the connections and the role of panel zone in transferring the bending moment from beam to column based on the results of numerical analysis, verified in this research for I-beam to built-up box-column connections without continuity plates as well as the models verified and reported by Saneei Nia et al. for similar connections with continuity plates.

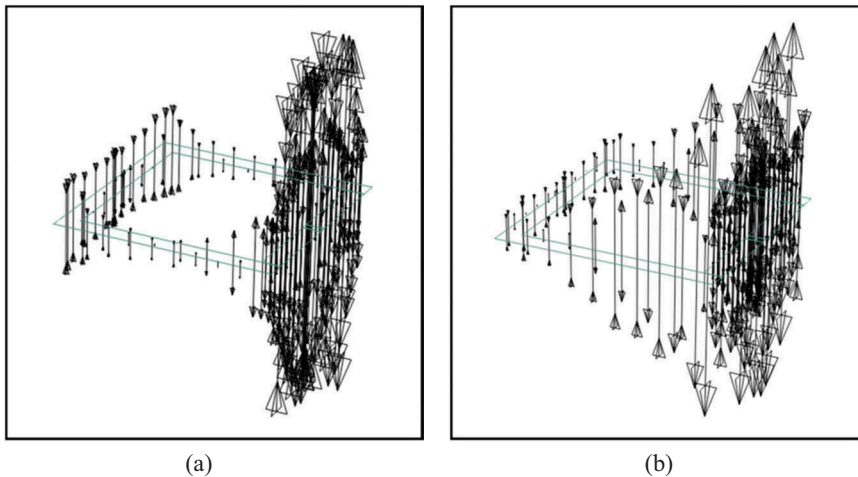


Figure 14. Stress (Pa) through column flanges for specimen Sp-L in the connection beam flange of one-way I-beam to box-column connection: (a) with continuity plates and (b) without continuity plates.

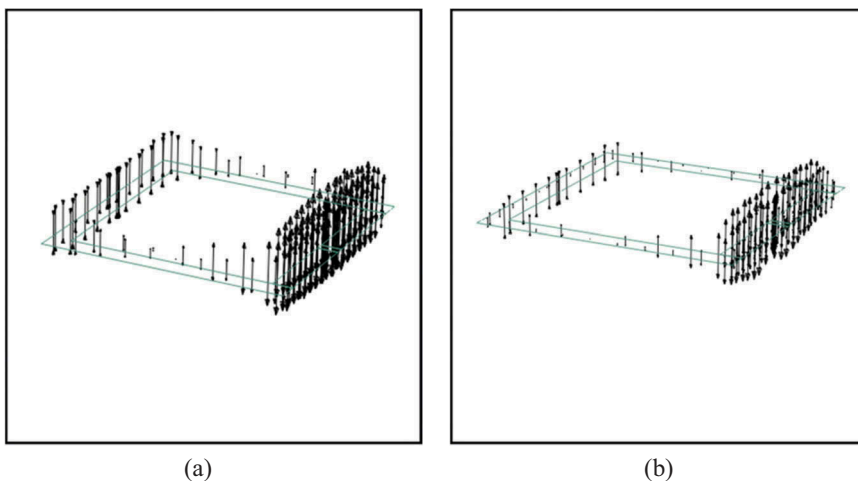


Figure 15. Stress (Pa) through column flanges for specimen Sp-L with a distance from panel zone of one-way I-beam to box-column connection: (a) with continuity plates and (b) without continuity plates.

5. Discussion

According to Fig. 11, the continuity plates installed in the panel zone of beam to column rigid connections cause the transmission of beam moment to column through integrating the panel zone components. The transmitted moment causes the column flanges to be in tensile and compressive statuses. In fact, the presence of continuity plates in the panel zone will involve considerable bending capacity of the column in the moment transmitted from the beam. Based on Figs. 12–15, in the panel zones with continuity plates, the beam loads are mostly transmitted to these plates and through them, to their whole components. The tension and compression transmitted to the panel zone create a bending moment under which the column flanges are subjected to compression and tension. The panel zones of the connections without continuity plates are under moment due to the tension and compression created in the column webs. Such moments are transmitted to the column flanges in the form of tension and compression.

RI has been calculated for I-beam to box-column connection in WUF-W rigid connection with and without continuity plates. Based on the obtained results, brittle rupture potential is higher in the connections without continuity plates than in those with continuity plates. In a certain drift angle, column flange deformation is more significant in the connection without continuity plates than in that with continuity plates. The presence of these continuity plates in the connections results in limited column flange deformation as well as more uniform distribution of the strain occurring in the beam flange. Therefore, higher potential of brittle fracture is expected in the connections without continuity plates. Based on the experimental observations, the crack occurs in the lateral regions of beam flange in its connection to the column flange, and finally, the connection fails in the region of the cracks. It should be noted that the connection failure occurs in the direction that groove weld has been executed for connecting beam flange to column flange by fillet backing weld. Assessing the RI in this research shows that this kind of welding has a higher potential of brittle rupture than groove weld with back plate.

6. Conclusion

In this research, FEA was conducted for the rigid connections of I-beam to box-column by focusing on the panel zone with and without continuity plates in WUF-W connections. The obtained results were compared with those of the experimental tests conducted on the connections without continuity plates. The drawn conclusions based on the experimental and numerical assessments of the tested specimens are briefly summarized as follows. The obtained results were based on a limited number of experimental tests. Also, the scope of the study was limited and wide investigations are needed to prove the results more confidently.

- (1) Based on the comparison between the finite element and the experimental results, the specimens were designed without continuity plates in a way to withstand permissible strength degradation and reach total story drift of 0.06 radians, satisfying AISC seismic provisions for prequalified connections.
- (2) Investigations into Sp-S specimen for different thicknesses of column flange calculated by Eqs. (3) and (4) derived from the study by Jahanbakhti, Fanaie, and Rezaeian

(2017) showed that the proposed mechanism and mathematical calculations were effectively reliable in estimating the column flange local bending capacity as well as identifying the requirement of continuity plates in a box-column in connection with an I-beam. Also, according to experimental reports, the thickness values of column flange in the panel zone obtained from experimental tests of Sp-S, Sp-M, and Sp-L specimens were equal to, lower than, and higher than those calculated by Eq. (2), respectively. In Sp-S and Sp-L specimens, the cracks were formed at a drift angle of 0.04 radians and in Sp-M sample, the crack was formed at a drift angle of 0.03 radians. Although the Sp-M sample satisfied the AISC criterion for SMRFs regarding the minimum strength at drift angle of 0.04 radians and acceptable strength loss, according to FEMA-350, such connection does not have reliable behavior. Therefore, Eq. (2) is verified for controlling local bending of the box-column flange and the necessity of installing continuity plates in the panel zone of box-column.

- (3) Based on the analytical studies, the portion of bending moment of column flange in connection without continuity plates was larger than that in the connection with continuity plates.
- (4) The relative results showed that the mechanism of force transmission from beam to column in the panel zone without continuity plates was approximately same as that in the panel zone with continuity plates.
- (5) Connecting beam flange to column flange through groove weld with fillet weld as the backing had higher potential for brittle fracture than that through groove weld by installing plate as the backing.
- (6) The implementation of groove welds with back plate is highly recommended for seismic design rather than groove welds with back fillet weld.

References

- AISC-341-10. 2010 Seismic provisions for structural steel buildings. AISC.
- Castro, J. M., F. J. Dávila-Arbona, and A. Y. Elghazouli. 2008. Seismic design approaches for panel zones in steel moment frames. *Journal of Earthquake Engineering* 12 (S1): 34–51. doi: [10.1080/13632460801922712](https://doi.org/10.1080/13632460801922712).
- Chen, C. C., C. C. Lin, and C. H. Lin. 2006. Ductile moment connections used in steel column-tree moment-resisting frames. *Journal of Constructional Steel Research* 793–801. doi: [10.1016/j.jcsr.2005.11.012](https://doi.org/10.1016/j.jcsr.2005.11.012).
- Chen, C. C., C. C. Lin, and C. L. Tsai. 2004. Evaluation of reinforced connections between steel beams and box columns. *Journal of Engineering Structures* 1889–904. doi: [10.1016/j.engstruct.2004.06.017](https://doi.org/10.1016/j.engstruct.2004.06.017).
- Chou, C. C., and C. K. Jao. 2010. seismic rehabilitation of welded steel beam-to-box column connection utilizing internal flange stiffeners. *Earthquake Engineering Research Institute*. 26 (4): 927–950. doi:[10.1193/1.3480275](https://doi.org/10.1193/1.3480275).
- Ghobadi, M. S., M. Ghassemieh, A. Mazroi, and A. Abolmaali. 2009. Seismic performance of ductile welded connections using T-stiffener. *Journal of Constructional Steel Research* 766–75. doi: [10.1016/j.jcsr.2008.05.007](https://doi.org/10.1016/j.jcsr.2008.05.007).
- Goswami, R., and C. V. R. Murty. 2010. Externally reinforced welded I-beam-to-box-column seismic connection. *Journal of Engineering Mechanics*. doi: [10.1061/\(ASCE\)0733-9399\(2010\)136:1\(23\)](https://doi.org/10.1061/(ASCE)0733-9399(2010)136:1(23)).
- Iannone, F., M. Latour, V. Piluso, and G. Rizzano. 2011. Experimental analysis of bolted steel beam-to-column connections: Component identification. *Journal of Earthquake Engineering* 15 (2): 214–44. doi: [10.1080/13632461003695353](https://doi.org/10.1080/13632461003695353).

- Jahanbakhti, E., N. Fanaie, and A. Rezaeian. 2017. Experimental investigation of panel zone in rigid beam to box column connection. *Journal of Constructional Steel Research* 180–91. doi: [10.1016/j.jcsr.2017.06.025](https://doi.org/10.1016/j.jcsr.2017.06.025).
- Kang, C. H., K. J. Shin, Y. S. Oh, and T. S. Moon. 2001. Hysteresis behavior of CFT column to H-beam connections with external T-stiffener and penetrated elements. *Engineering Structures* 1194–201. doi: [10.1016/S0141-0296\(00\)00119-X](https://doi.org/10.1016/S0141-0296(00)00119-X).
- Kiamanesh, R., A. Abolmaali, and M. Ghassemieh. 2010. The effect of stiffeners on the strain patterns of the welded connection zone. *Journal of Constructional Steel Research* 19–27. doi: [10.1016/j.jcsr.2009.07.010](https://doi.org/10.1016/j.jcsr.2009.07.010).
- Kim, Y. J., and S. H. Oh. 2007. Effect of the moment transfer efficiency of a beam web on deformation capacity at box column-to-H beam connections. *Journal of Constructional Steel Research* 24–36. doi: [10.1016/j.jcsr.2006.02.009](https://doi.org/10.1016/j.jcsr.2006.02.009).
- Korol, R. M., A. Ghobarah, and S. Mourad. 1993. Blind bolted W-shaped beam to HSS columns. *Journal of Engineering Structures*. ASCE. doi:[10.1061/\(ASCE\)0733-9445\(1993\)119:12\(3463\)](https://doi.org/10.1061/(ASCE)0733-9445(1993)119:12(3463)).
- Kurobane, Y. 2002. Connections in tubular structures. *Progress in Structural Engineering and Materials* 35–45. doi: [10.1002/pse.102](https://doi.org/10.1002/pse.102).
- Latour, M., V. Piluso, and G. Rizzano. 2011. Cyclic modeling of bolted beam-to-column connections: Component approach. *Journal of Earthquake Engineering* 15 (4): 537–63. doi: [10.1080/13632469.2010.513423](https://doi.org/10.1080/13632469.2010.513423).
- Mirghaderi, S. R., and M. Moradi. 2006. Seismic behavior of panel zones in beam to column connections with non-planar webs in moment resistance steel frames. 4th International Conference on Earthquake Engineering Taipei, Taipei, Taiwan.
- Mirghaderi, S. R., S. Torabian, and F. Keshavarzi. 2010. I-beam to box-column connection by a vertical plate passing through the column. *Engineering Structures* 2034–48. doi: [10.1016/j.engstruct.2010.03.002](https://doi.org/10.1016/j.engstruct.2010.03.002).
- Nia, Z. S., M. Ghassemieh, and A. Mazroi. 2013. WUF-W connection performance to box column subjected to uniaxial and biaxial loading. *Journal of Constructional Steel Research* 88: 90–108. doi:[10.1016/j.jcsr.2013.04.008](https://doi.org/10.1016/j.jcsr.2013.04.008).
- Park, J. W., S. M. Kang, and S. C. Yang. 2005. Experimental studies of wide flange beam to square concrete-filled tube column joints with stiffening plated around the column. *Journal of Engineering Structures*. ASCE. doi:[10.1061/\(ASCE\)0733-9445\(2005\)131:12\(1866\)](https://doi.org/10.1061/(ASCE)0733-9445(2005)131:12(1866)).
- Ricles, J. M., J. W. Fisher, L. W. Lu, and E. J. Kaufmann. 2002. Development of improved welded moment connections for earthquake-resistant design. *Journal of Constructional Steel Research* 565–604. doi: [10.1016/S0143-974X\(01\)00095-5](https://doi.org/10.1016/S0143-974X(01)00095-5).
- Shanmugam, N. E., and L. C. Ting. 1995. Welded interior box-column to I-beam connections. *Journal of Structural Engineering*. ASCE. doi:[10.1061/\(ASCE\)0733-9445\(1995\)121:5\(824\)](https://doi.org/10.1061/(ASCE)0733-9445(1995)121:5(824)).
- Shanmugam, N. E., and L. C. Ting. 1991. Behavior of I-beam to box-column connections stiffened externally and subjected to fluctuating loads. *Journal of Constructional Steel Research* 129–48. doi: [10.1016/0143-974X\(91\)90016-T](https://doi.org/10.1016/0143-974X(91)90016-T).
- Shin, K. J., Y. J. Kim, and Y. S. Oh. 2008. Seismic behavior of composite concrete-filled tube column-to-beam moment connections. *Journal of Constructional Steel Research* 118–27. doi: [10.1016/j.jcsr.2007.04.001](https://doi.org/10.1016/j.jcsr.2007.04.001).
- Tanaka, N. 2003. Evaluation of maximum strength and optimum haunch length of steel beam-end with horizontal haunch. *Journal of Engineering Structures* 229–39. doi: [10.1016/S0141-0296\(02\)00146-3](https://doi.org/10.1016/S0141-0296(02)00146-3).
- Torabian, S., S. R. Mirghaderi, and F. Keshavarzi. 2012. Moment-connection between I-beam and built-up square column by a diagonal through plate. *Journal of Constructional Steel Research* 385–401. doi: [10.1016/j.jcsr.2011.10.017](https://doi.org/10.1016/j.jcsr.2011.10.017).
- Wheeler, A. T., M. J. Clarke, and G. J. Hancock. 2001. FE modeling of four-bolt tubular moment end-plate connections. *Journal of Engineering Structures*. 126 (7). doi:[10.1061/\(ASCE\)0733-9445\(2000\)126:7\(816\)](https://doi.org/10.1061/(ASCE)0733-9445(2000)126:7(816)).
- Wheeler, A. T., M. J. Clarke, G. J. Hancock, and T. M. Murray. 1998. Design model for bolted moment end plate connections joining rectangular hollow sections. *Journal of Engineering Structures*. ASCE. doi:[10.1061/\(ASCE\)0733-9445\(1998\)124:2\(164\)](https://doi.org/10.1061/(ASCE)0733-9445(1998)124:2(164)).